Theoretical Calculation of Structures and Proton Transfer in Hydrated Ammonia−Hydrogen Chloride Clusters

Toshio Asada,* Seisuke Takitani, and Shiro Koseki

Department of Chemistry, Osaka Prefecture University, 1-1 Gakuen-cho, Sakai-city, Osaka 599-8531, Japan

Received: September 9, 2004; In Final Form: December 9, 2004

Ab initio molecular orbital calculations have been performed to investigate the structures and quantum effects of the proton motion in NH_3:HCl:$(H_2O)_n$ ($n = 0-3$) clusters using a MP2/aug-cc-pVDZ level of theory. Three new stable structures and one transition-state structure are investigated for these clusters. The detailed analyses of the intermolecular interactions suggest that three-body interactions play an important role to determine the relative stability in each size of cluster. The quantum effects of the proton motion result in frequency shifts for proton-stretching modes. Our one-dimensional and two-dimensional models fairly closely reproduce the experimental proton-stretching vibrational frequency of the NH_3:HCl cluster. The most stable isomer for $n = 1$ has a proton-transfer structure, which is weakened by the quantum effects of the proton motion.

1. Introduction

Proton-transfer reactions play an important role in many molecular systems, such as clusters,[1−13] liquids,[14] crystals,[15] and so forth. They are of particular interest with respect to quantum phenomena. The proton-transfer processes are also related to proton-tunneling effects or proton disorders in hydrogen-bonded systems observed in biomolecules.

It is usually the case that proton motion cannot be treated classically[16] because the mass of the proton is so small. The quantum effects of the proton motion relax the localization effect of the proton position, and the wave function of the ground state sometimes broadly spreads. For example, we have previously studied the $N_2H_7^+$ cluster[12] using quantum wave-packet dynamics. If the quantum effects of the proton motion are taken into account, $N_2H_7^+$ is predicted to have D_{3d} symmetry, not C_{3v} symmetry. From the spectrum of $N_2H_7^+$, one deduces D_{3d} symmetry.

The ammonia−hydrogen chloride cluster is a simple and typical strong acid−base pair. Thus, it is an important aid to the understanding of a wide variety of chemical reactions, such as proton transfers in biological systems. Previous theoretical and experimental studies demonstrated that the gas-phase NH_3:HCl system exists as a hydrogen-bonded complex.[17,18] In water solution, the NH_4^+:Cl^- ion pair is more stable. Cazar and coworkers[9] studied binding energies and one-dimensional potential-energy curves along the proton-transfer pathway of NH_3:HCl:$(H_2O)_n$ ($n = 0-3$) at the MP2/6-311++G(d,p) level of theory. They found that proton transfer is energetically favorable for $n = 2$. Latajka and Biczysko[1] confirmed this finding in calculations at the B3LYP/6-311++G(d,p) level. However, in a successive study, Li et al.[13] concluded that the basis set should be larger than 6-311++G(d,p) for theoretical research on proton transfer in NH_3:HCl:H_2O. The global energy-minimum structure at the MP2/6-311++G(d,p) level is different from what is found using larger basis sets.[13] They have recalculated stable structures at the B3LYP/d-aug-cc-pVDZ level of theory and found that a proton transfer from HCl to NH_3 occurs at the $n = 1$ cluster. However, the quantum effect of the bound proton was not taken into account.

For the $n = 0$ cluster, Del Bene and Jordan[11] investigated the effect of proton delocalization using the MP2/aug-cc-pVDZ level of theory. They found that the classical harmonic treatment leads to a significant overestimation of the experimental proton-stretching frequency.

This paper reports stable structures of NH_3:HCl:$(H_2O)_n$ ($n = 0-3$) clusters determined from ab initio molecular orbital (MO) calculations. We first discuss the structures and energies of these clusters. The intermolecular interaction within a given cluster was decomposed into one-body, two-body, three-body, and so forth terms. The relative importance of these various terms is discussed. Finally, the quantum effect of delocalization of the bound proton was investigated by diagonalizing the model Hamiltonian. On the basis of wave functions thereby computed, a discussion of the effects of proton delocalization on the structures of the complexes is presented.

2. Method

2.1. Structures and Interaction Energies. All geometry optimizations of HCl:NH_3:$(H_2O)_n$ ($n = 0-3$) have been carried out using Gaussian98.[19] Normal-mode analyses were performed to verify that optimized structures are either true minima or transition states on the potential-energy surface. In the present paper, second-order Moller−Plesset (MP2) theories with aug-cc-pVDZ basis sets[20−22] were applied to obtain potential-energy surfaces. These basis sets are Dunning's correlation-consistent polarized-valence double-ζ basis sets augmented by diffuse functions on non-hydrogen atoms. They are known to improve energetics for hydrogen-bonded systems.[23]

The intermolecular interaction energy E_{int} can be expanded as

$$E_{int} = \sum_i \Delta E^{(1)}[i] + \sum_{i>j} \Delta E^{(2)}[i:j] + \sum_{i>j>k} \Delta E^{(3)}[i:j:k] + \sum_{i>j>k>l} \Delta E^{(4)}[i:j:k:l] + \ldots \quad (1)$$

* Author to whom correspondence should be addressed. E-mail: asada@ms.cias.osakafu-u.ac.jp.

10.1021/jp045933m CCC: $30.25
Published on Web 02/09/2005

$$\Delta E^{(1)}[i] = E_i^{\text{comp}}[i] - E^{\text{vac}}[i] \tag{2}$$

$$\Delta E^{(2)}[i:j] = E^{\text{comp}}[i:j] - E^{\text{comp}}[i] - E^{\text{comp}}[j] \tag{3}$$

$$\Delta E^{(3)}[i:j:k] = E^{\text{comp}}[i:j:k] - \sum_{l\in i,j,k} E^{\text{comp}}[l] - \sum_{\substack{l>m \\ l,m\in i,j,k}} \Delta E^{(2)}[l:m] \tag{4}$$

$$\Delta E^{(4)}[i:j:k:l] = E^{\text{comp}}[i:j:k:l] - \sum_{m\in i,j,k,l} E^{\text{comp}}[m] - \sum_{\substack{m>n \\ m,n\in i,j,k,l}} \Delta E^{(2)}[m:n] - \sum_{\substack{m>n>p \\ m,n,p\in i,j,k,l}} \Delta E^{(3)}[m:n:p] \tag{5}$$

where $\Delta E^{(1)}[i]$ is the deformation energy of the molecule i. $E^{\text{vac}}[i]$ is the energy of an isolated molecule i, and $E^{\text{comp}}[i:j:k:...]$ is the energy of molecules i, j, k, ... when they are part of the complex. In these expansions, $\Delta E^{(2)}[i:j]$, $\Delta E^{(3)}[i:j:k]$, and $\Delta E^{(4)}[i:j:k:l]$ are two-, three-, and four-body-interaction energies, respectively. Three-body, four-body, and so forth interactions are referred to as many-body interactions.

2.2. Quantum Effects of the Proton Motion. To investigate the quantum effects of the bound proton between the nitrogen and chloride atoms, we have used one-dimensional (1-D) and two-dimensional (2-D) potential surfaces for $n = 0$ and 1 clusters. For $n = 2$ and 3 clusters, only the 1-D model has been applied because it is very time consuming to generate 2-D potential surfaces, given our computational resources. In the 2-D model, the two coordinates considered are the H−Cl bond length and the N−Cl bond length for $n = 0$. The N−H bond length and the N−Cl bond length were used for $n = 1$. In the 1-D model, potential-energy curves have been generated along the proton-transfer minimum-energy path.

In the 2-D model, components of the $n \times n$ discrete representation of Hamiltonian matrix $\mathscr{H}_{l,m}$ can be written as

$$\mathscr{H}_{l,m} = \frac{\hbar^2}{(\Delta q_x)^2} + \frac{\hbar^2}{(\Delta q_y)^2} \qquad (\text{if } l = m) \tag{6}$$

$$\mathscr{H}_{l,m} = \frac{-\hbar^2}{2(\Delta q_i)^2} \qquad (\text{if 1 is a neighboring grid of } m;\ i \in x, y) \tag{7}$$

$$\mathscr{H}_{l,m} = 0 \qquad (\text{in other cases}) \tag{8}$$

In these equations, $\hbar$ is Planck's constant divided by 2π and Δq_x and Δq_y are intervals of the mass-weighted coordinate between neighboring grids along the x and y axis, respectively. Vibrational eigenfunctions and eigenvalues of the 1-D model were calculated using the same methods as those we have previously reported.[12]

3. Results and Discussion

3.1. Optimized Structures. Figure 1 shows stable structures and some interatomic distances. Total energies (E), binding energies (D_e), zero-point energies (ZPE), and ZPE-corrected binding energies (D_0) for these structures are summarized in Table 1. The D_e values are calculated by the difference between the energy of the molecular complex and the sum of energies of the isolated molecules. The water shared-ion-pair structure 1A has already been characterized by Li et al.[13] Structure 1A does not have C_s symmetry because the water molecule's dangling hydrogen atom is bent out of the mirror plane by 17°.

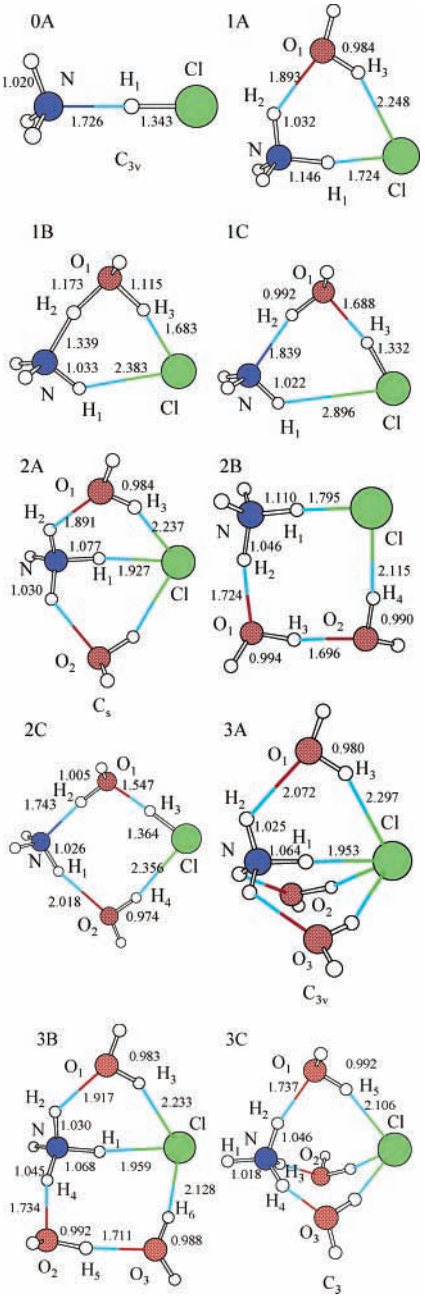

Figure 1. Optimized structures of NH_3:HCl:$(H_2O)_n$ clusters with some geometrical parameters. The geometrical parameters are determined with the MP2/aug-cc-pVDZ method. These structures are confirmed to be real minima by evaluating the harmonic frequencies.

Table 1 indicates considerable basis-set dependence of the calculated D_e values. This basis-set dependence is probably due to basis-set superposition error (BSSE). The correlation-consistent aug-cc-pVDZ basis sets systematically extend the atomic radial (R) and angular spaces. Thus, the effects of the BSSE on the intermolecular interactions can be shown to be small for various properties[24,25] if such basis sets are used. Indeed, the present structure, 1A, using the MP2/aug-cc-pVDZ method (127 basis functions; $R_{N-H1} = 1.146$ Å, $R_{H1-Cl} = 1.724$ Å), is very close to the structure using larger basis sets such as MP2/d-aug-cc-pVDZ (178 basis functions) and MP2/6-311++G-(2df,2p) (170 basis functions) results[13] ($R_{N-H1} = 1.145$ Å, $R_{H1-Cl} = 1.724$ Å and $R_{N-H1} = 1.141$ Å, $R_{H1-Cl} = 1.718$ Å, respectively). In the B3LYP/d-aug-cc-pVDZ structure obtained by Li et al.,[13] N−H_1 and H_1−Cl distances are 0.005 and 0.014 Å longer than the MP2/d-aug-cc-pVDZ results, respectively.

TABLE 1: MP2 Total Energies *E* (Hartree), Binding Energies D_e (kcal/mol), MP2 Zero-Point Energies ZPE (kcal/mol), and ZPE-Corrected Binding Energies D_0 (kcal/mol)

	E^a	E^b	$D_e{}^a$	$D_e{}^b$	ZPE^a	ZPE^b	$D_0{}^a$	$D_0{}^b$
0A	−516.672 45	−516.675 20	−9.88	−9.26	2.32	2.61	−7.56	−6.65
1A	−592.948 95	−592.962 56	−19.66	−17.07	6.02	4.51	−13.64	−12.56
1B	−592.934 46		−10.57		3.62		−6.95	
1C	−592.944 98		−17.17		4.65		−12.52	
2A	−669.232 27	−668.451 59	−33.72	−30.44	9.31	9.83	−24.41	−20.61
2B	−669.232 23		−33.70		9.32		−24.38	
2C	−669.220 26		−26.18		6.55		−19.63	
3A	−745.512 67	−745.553 28	−45.95	−42.72	11.43	11.58	−34.52	−31.14
3B	−745.515 63		−47.81		12.10		−35.71	
3C	−745.517 51		−48.99		12.60		−36.39	

[a] aug-cc-pVDZ basis set. [b] 6-311++G(d,p) basis set.[9]

TABLE 2: Sums of Deformation Energies $\sum\Delta E^{(1)}$ and Two-Body $\sum\Delta E^{(2)}$, Three-Body $\sum\Delta E^{(3)}$, Four-Body $\sum\Delta E^{(4)}$, and Five-Body $\sum\Delta E^{(5)}$ Interaction Energies (in kcal/mol)

	$\sum\Delta E^{(1)}$	$\sum\Delta E^{(2)}$	$\sum(\Delta E^{(1)}+\Delta E^{(2)})$	$\sum\Delta E^{(3)}$	$\sum\Delta E^{(4)}$	$\sum\Delta E^{(5)}$	$D_e{}^a$
0A	1.07	−10.95	−9.88				−9.88
1A	128.02	−154.23	−26.21	6.55			−19.66
1C	1.15	−15.42	−14.27	−2.90			−17.17
2A	124.45	−169.24	−44.79	11.57	−0.50		−33.72
2B	125.75	−166.46	−40.71	6.90	0.11		−33.70
2C	2.94	−21.45	−18.51	−7.02	−0.65		−26.18
3A	123.61	−185.83	−62.22	17.56	−1.42	0.13	−45.95
3B	124.22	−183.99	−59.77	12.74	−0.81	0.03	−47.81
3C	123.75	−184.40	−60.65	11.92	−0.42	0.16	−48.99

[a] ZPE non-corrected binding energies using aug-cc-pVDZ basis sets.

The new isomer, 1C, was found in the present study. Its energy is 2.49 kcal/mol higher than that of isomer 1A (see the D_e values in Table 1). However, D_0 values of 1A and 1C become −13.64 and −12.52 kcal/mol, respectively; that is, the ZPE correction reduces the energy difference to 1.12 kcal/mol. Clearly, structure 1C is a hydrogen-bonded molecular pair. The transition-state structure 1B indicates concerted motion of H_2 and H_3 in the formation of 1A from 1C. The D_0 energy of this transition state is estimated to be 5.57 kcal/mol higher than that of 1C. This implies that 1C is kinetically rather stable at low temperature. Following the statistical Boltzmann weight factor, we can estimate the probability of findings of 1C to be about 13.4% at the room temperature of 300 K.

Three isomers were found for $n = 2$ clusters. In the most stable isomer, 2A, the hydrogen-bonding pattern is similar to that of 1A. The isomer 2B may be regarded as an eight-membered ring. The difference of D_0 energies between 2A and 2B was found to be negligibly small. The higher-energy isomer is clearly a hydrated NH_3:HCl complex. D_0 of 2C is 4.78 kcal/mol higher than that of 2A. For $n = 3$ clusters, we found a new configuration, 3C, which is the most stable isomer in $n = 3$ clusters.

3.2. Intermolecular Interactions. Table 2 lists sums of deformation energies and two-, three-, four-, and five-body-interaction energies of each stable isomer. Components of these many-body interactions are summarized in Table 3. Four- and five-body interactions make small contributions to total D_e values except in the case of structure 3A; the total four-body interaction is −1.42 kcal/mol, 3.1% of D_e. The relative stability order can be roughly explained by the deformation, pair, and three-body interactions. Considering up to pair additive interactions, the relative stability order cannot be reproduced. For example, $\sum(\Delta E^{(1)} + \Delta E^{(2)})$ values indicate that 3A is the most stable of the $n = 3$ clusters. If three-body interactions are taken into account, structure 3C is found to be the most stable. Thus, the three-body interactions must be included in order to obtain the correct relative stabilities.

The sums of three-body-interaction energies, $\sum\Delta E^{(3)}$, are positive values except for those of isomers 1C and 2C, as seen in Table 2. Following the definition of three-body-interaction energy given in eq 3, the positive value indicates that the calculated interaction energy of the isomer becomes less stable, taking three-body interactions into account, than that of the pair additive approximation. Each molecule that is a part of isomers 1C and 2C has two hydrogen bonds and behaves as a proton donor and, spontaneously, as a proton acceptor. These "push-and-pull" cooperative effects of protons usually have negative energy contributions to the sum of three-body-interaction energies. Indeed, component analyses in Table 3 show that three-body-interaction energies $\Delta E^{(3)}[M_i{:}M_j{:}M_k]$ are positive values if component molecule M_i, M_j, or M_k has characteristics of either a "two"-proton donor or a "two"-proton acceptor. For example, $\Delta E^{(3)}[NH_4{}^+{:}Cl^-{:}H_2O]$ in 2A is 4.82 kcal/mol. In this moiety, H_1 and H_2 atoms in the $NH_4{}^+$ ion bind to the oxygen atom in H_2O and the Cl^- ion, respectively. Therefore, $NH_4{}^+$ and Cl^- ions can be considered as a "two"-proton donor and a "two"-proton acceptor, respectively. Thus, $\Delta E^{(3)}[NH_4{}^+{:}Cl^-{:}H_2O]$ in 2A becomes a positive value. This simple rule seems to fail only for $\Delta E^{(3)}[NH_4{}^+{:}Cl^-{:}H_2O]$ in 3C, which is 0.45 kcal/mol. However, two symmetric protons, H_3 and H_4, bind directly to the chloride ion; therefore, the ammonia and chloride ions have characteristics of a "two"-proton donor and a "two"-proton acceptor, respectively. Because there are two large negative three-body components in 2B, $\Delta E^{(3)}[NH_4{}^+{:}O_1{:}O_2]$ and $\Delta E^{(3)}[Cl^-{:}O_1{:}O_2]$, the D_e values become very close to each other between isomers 2A and 2B.

3.3. Quantum Effects of the Proton Motion. We now discuss the quantum effects of the proton motion using model potential surfaces. Isomers 1C and 2C are unfavorable at room temperature considering statistical Boltzmann weight factors, as we mentioned above. Unfortunately, we have to treat more than two mode couplings for isomers 1C, 2C, and 3C. As we will discuss later, the potential-energy curve for the proton motion is more flat in 1A than in 1C, and the required energy from 1C to 1A is large, that is, 5.57 kcal/mol. Thus, the concerted proton motion is more important in 1C than in 1A. There are symmetrical protons in 2C and 3C. In these three isomers (1C, 2C, and 3C), we must consider double proton transfers to provide sufficient reliable information, where two protons should be treated quantum mechanically; therefore, they require quite-large computational resources. For these reasons, we will pay attention to single proton-transfer processes in 0A, 1A, 2A, 2B, 3A, and 3B, which will be used for dynamic analyses based on 1-D models. Dynamic behaviors of 0A and 1A are also analyzed using 2-D models.

TABLE 3: Components of Deformation Energies $\Delta E^{(1)}[M_i]$, Two-Body $\Delta E^{(2)}[M_i:M_j]$, Three-Body $\Delta E^{(3)}[M_i:M_j:M_k]$, and Four-Body $\Delta E^{(4)}[M_i:M_j:M_k:M_l]$ Interaction Energies in NH_3:HCl:$(H_2O)_n$ ($n = 0-3$) Clusters (in kcal/mol)

	$\Delta E^{(1)}[M_i]$[a]	M_i[b]	$\Delta E^{(2)}[M_i:M_j]$[c]	$M_i:M_j$[b]	$\Delta E^{(3)}[M_i:M_j:M_k]$[d]	$M_i:M_j:M_k$[b]	$\Delta E^{(4)}[M_i:M_j:M_k:M_l]$[e]	$M_i:M_j:M_k:M_l$[b]
0A	0.01	NH_3	−10.95	NH_3:HCl				
	1.05	HCl						
1A	−204.22	NH_4^+	−131.59	NH_4^+:Cl^-	6.55	NH_4^+:Cl^-:H_2O		
	331.99	Cl^-	−11.58	NH_4^+:H_2O				
	0.25	H_2O	−11.07	Cl^-:H_2O				
1C	0.01	NH_3	−2.67	NH_3:HCl	−2.90	NH_3:HCl:H_2O		
	0.69	HCl	−6.78	NH_3:H_2O				
	0.45	H_2O	−5.96	HCl:H_2O				
2A	−208.05	NH_4^+	−123.22	NH_4^+:Cl^-	4.82	NH_4^+:Cl^-:H_2O	−0.50	NH_4^+:Cl^-:H_2O:H_2O
	331.99	Cl^-	−11.83	NH_4^+:H_2O	1.10	NH_4^+:H_2O:H_2O		
	0.26	H_2O	−11.60	Cl^-:H_2O	0.83	Cl^-:H_2O:H_2O		
			0.83	H_2O:H_2O				
2B	−207.07	NH_4^+	−127.52	NH_4^+:Cl^-	7.29	NH_4^+:Cl^-:O_1	0.11	NH_4^+:Cl^-:O_1:O_2
	331.99	Cl^-	−17.81	NH_4^+:O_1	5.36	NH_4^+:Cl^-:O_2		
	0.51	O_1	−1.59	NH_4^+:O_2	−2.60	NH_4^+:O_1:O_2		
	0.32	O_2	−1.02	Cl^-:O_1	−3.15	Cl^-:O_1:O_2		
			−14.05	Cl^-:O_2				
			−4.48	O_1:O_2				
2C	0.03	NH_3	−2.10	NH_3:HCl	−0.55	NH_3:HCl:O_1	−0.65	NH_3:HCl:O_1:O_2
	1.92	HCl	−2.71	NH_3:O_1	−3.72	NH_3:HCl:O_2		
	0.04	O_1	−6.82	NH_3:O_2	−1.09	NH_3:O_1:O_2		
	0.95	O_2	−1.96	Cl^-:O_1	−1.67	HCl:O_1:O_2		
			−6.31	Cl^-:O_2				
			−1.54	O_1:O_2				
3A	−208.84	NH_4^+	−121.90	NH_4^+:Cl^-	4.35	NH_4^+:Cl^-:H_2O	−0.40	NH_4^+:Cl^-:H_2O:H_2O
	331.99	Cl^-	−10.81	NH_4^+:H_2O	0.72	NH_4^+:H_2O:H_2O	−0.13	NH_4^+:H_2O:H_2O:H_2O
	0.16	H_2O	−11.26	Cl^-:H_2O	0.80	Cl^-:H_2O:H_2O	−0.11	Cl^-:H_2O:H_2O:H_2O
			0.76	H_2O:H_2O	−0.04	H_2O:H_2O:H_2O		
3B	−208.74	NH_4^+	−121.82	NH_4^+:Cl^-	4.59	NH_4^+:Cl^-:O_1	−0.52	NH_4^+:Cl^-:O_1:O_2
	331.99	Cl^-	−12.16	NH_4^+:O_1	6.26	NH_4^+:Cl^-:O_2	−0.43	NH_4^+:Cl^-:O_1:O_3
	0.24	O_1	−17.56	NH_4^+:O_2	4.63	NH_4^+:Cl^-:O_3	−0.12	NH_4^+:Cl^-:O_2:O_3
	0.44	O_2	−2.02	NH_4^+:O_3	1.44	NH_4^+:O_1:O_2	0.08	NH_4^+:O_1:O_2:O_3
	0.29	O_3	−11.58	Cl^-:O_1	0.08	NH_4^+:O_1:O_3	0.17	Cl^-:O_1:O_2:O_3
			−1.22	Cl^-:O_2	−2.45	NH_4^+:O_2:O_3		
			−14.10	Cl^-:O_3	0.08	Cl^-:O_1:O_2		
			0.39	O_1:O_2	0.99	Cl^-:O_1:O_3		
			0.64	O_1:O_3	−3.14	Cl^-:O_2:O_3		
			−4.57	O_2:O_3	0.26	O_1:O_2:O_3		
3C	−209.44	NH_4^+	−101.14	NH_4^+:Cl^-	0.45	NH_4^+:Cl^-:H_2O	−0.01	NH_4^+:Cl^-:H_2O:H_2O
	331.99	Cl^-	−15.52	NH_4^+:H_2O	2.29	NH_4^+:H_2O:H_2O	−0.24	NH_4^+:H_2O:H_2O:H_2O
	0.40	H_2O	−12.99	Cl^-:H_2O	1.26	Cl^-:H_2O:H_2O	−0.15	Cl^-:H_2O:H_2O:H_2O
			0.76	H_2O:H_2O	−0.08	H_2O:H_2O:H_2O		

[a] $\Delta E^{(1)}[M_i]$ is the deformation energy $\Delta E^{(1)}$ of molecular unit M_i. [b] O_1, O_2, and O_3 denote H_2O molecules including O_1, O_2, and O_3 atoms in Figure 1, respectively. [c] $\Delta E^{(2)}[M_i,M_j]$ is the two-body-interaction energy $\Delta E^{(2)}$ of molecular units M_i and M_j. [d] $\Delta E^{(3)}[M_i,M_j,M_k]$ is the three-body-interaction energy $\Delta E^{(3)}$ of molecular units M_i, M_j, and M_k. [e] $\Delta E^{(4)}[M_i,M_j,M_k,M_l]$ is the four-body-interaction energy $\Delta E^{(4)}$ of molecular units M_i, M_j, M_k, and M_l.

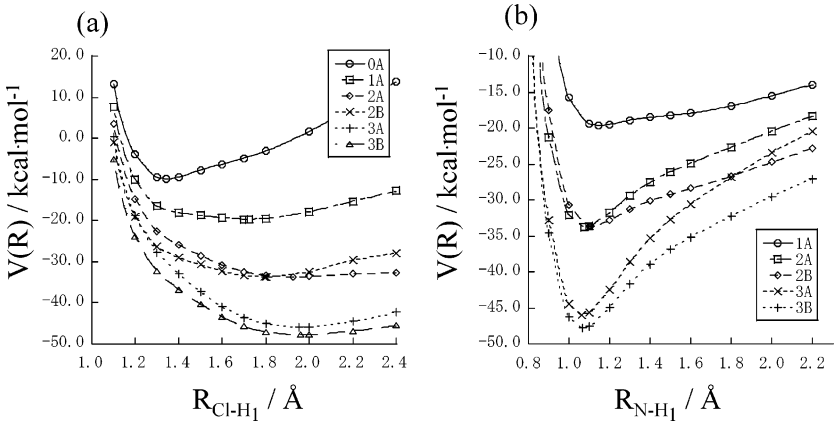

Figure 2. Potential-energy curves of the NH_3:HCl:$(H_2O)_n$ complex. (a) Potential curves along the R_{Cl-H1} distance. (b) Potential curves along the R_{N-H1} distance.

1-D potential-energy curves as a function of R_{Cl-H1} are illustrated in Figure 2a for each of the structures considered. D_e decreases with increasing hydration number n. Proton H_1 is bound to the chloride atom for structure 0A. The 1-D potential-energy curves for $n \geq 1$, in which the proton is bound to a nitrogen atom to make the ion pair form in stable structures, are rather flat at distances beyond the potential-energy minimum. In other words, NH_4^+ and Cl^- ions produced by proton-transfer

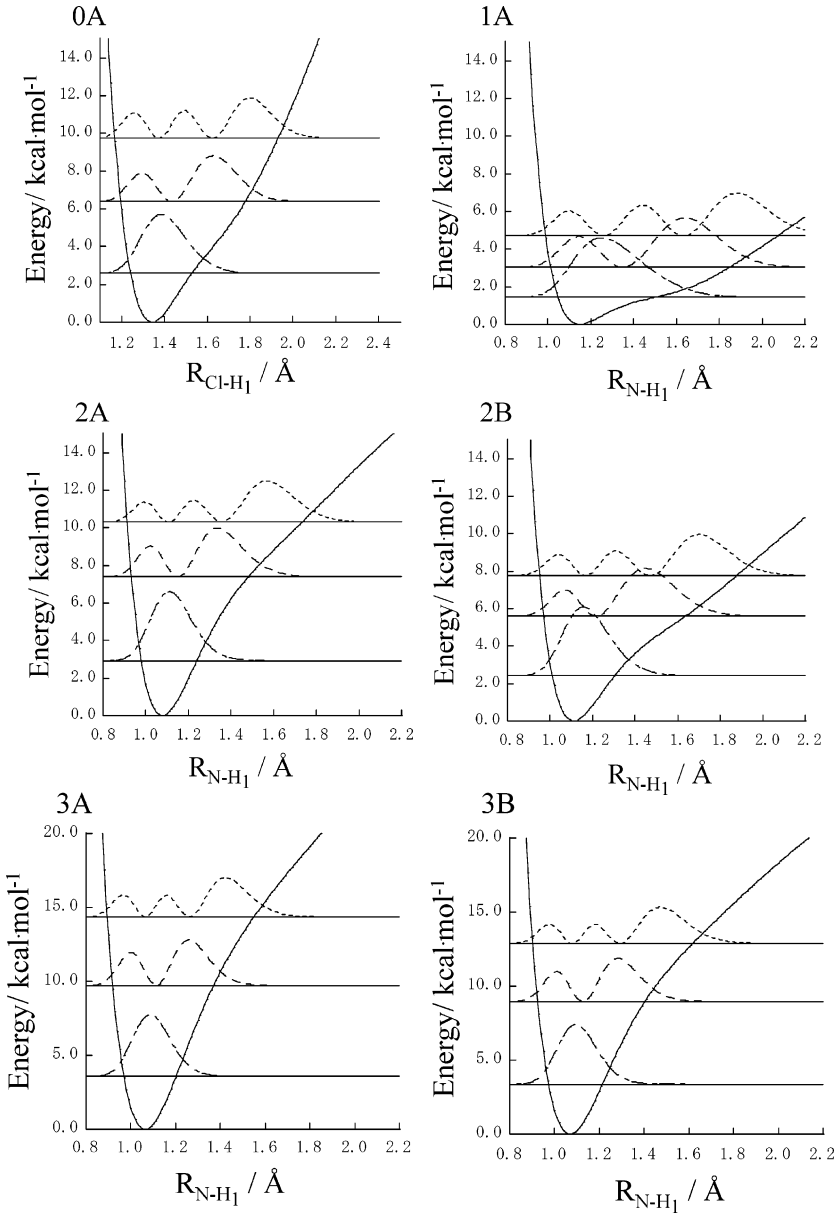

Figure 3. Potential-energy curves, probability distribution for the proton, that is, the squares of vibrational wave functions, and corresponding eigenvalues. The ground state, the first excited state, and the second excited state are depicted.

reactions may dissociate without high-energy barriers. To investigate the quantum effects of the proton motion using 1-D models for $n \geq 1$, R_{N-H1} is considered to be a more reasonable reaction coordinate for the proton transfer than R_{Cl-H1} because proton H_1 binds to N rather than Cl in its energy-minimum structures. These curves of potential energy as a function of R_{N-H1} are depicted in Figure 2b. Figure 3 illustrates proton distributions as a function of R_{N-H1}, which are given by the squares of vibrational wave functions, of the ground state and the first and second excited states for the proton nucleus with their corresponding eigenvalues superimposed on the MP2/aug-cc-pVDZ potential curves. The potential curve of 1A is quite anharmonic, and the corresponding wave function of the ground state has appreciable values for R_{N-H1} between 0.9 and 1.9 Å.

The partial optimization of 1A restricted to $R_{N-H1} = 1.6$ Å gives an R_{Cl-H1} value of nearly 1.4 Å. These distances are nearly the same as those for isomer 0A, which consists of NH_3 and HCl molecules. These results imply that proton H_1 accesses the proton-shared region[11] between nitrogen and chloride atoms in 1A even in its ground vibrational state. On the other hand, the proton does not penetrate into the proton-shared region for $n \geq 2$ clusters, because the probability function is negligible for R_{N-H1} equal to or greater than 1.6 Å.

Figures 4 and 5 illustrate 2-D calculated probability distributions for the ground state and the first excited states for 0A and 1A, respectively, superimposed on the MP2/aug-cc-pVDZ potential surfaces. There is weak mode coupling between the N−Cl and Cl−H_1 stretching modes for 0A, in contrast with those of 1A. In the latter complex, there is strong coupling between the N−Cl and N−H_1 stretching modes, especially in the first excited state. Table 4 summarizes expectation values of bond lengths $\langle R_{X-H1}\rangle_0$ and peak bond lengths r_{X-H1}^{max} for the ground-state wave functions calculated by using 1-D and 2-D models together with optimized equilibrium bond lengths r_{X-H1eq} obtained from ab initio MO calculations.

The calculated quantum results of the 1-D and 2-D models are close to each other for 0A and 1A. As one can see, in the 1-D models, quantum effects increase $\langle R_{X-H1eq}\rangle_0$ over r_{X-H1eq} by values ranging from 0.04 to 0.16 Å. In particular, the large shift is seen for isomer 1A, in which the expectation value for

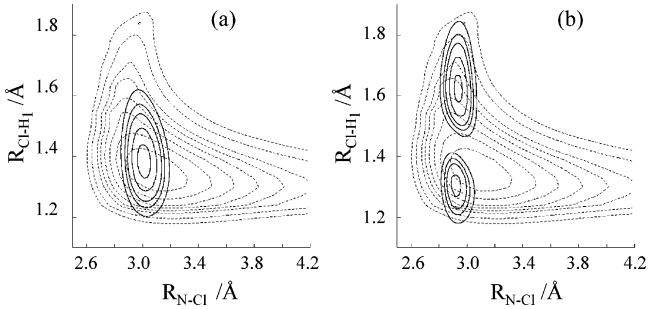

Figure 4. Squares of the wave functions for isomer 0A superimposed on the MP2/aug-cc-pVDZ potential surface. Potential-energy contours are at energies 1.0, 2.0, 3.0, 4.0, 5.0, 6.0, 8.0, and 10.0 kcal/mol above the global energy minimum. (a) The ground state and (b) the first excited state are shown.

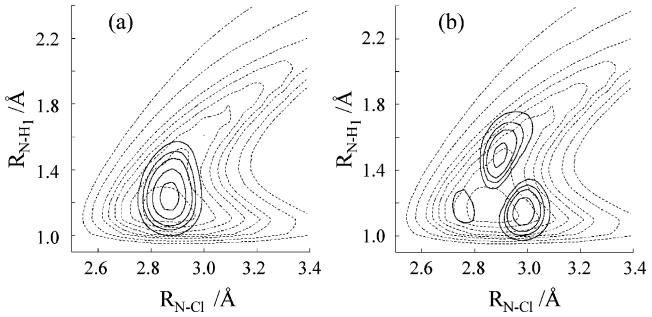

Figure 5. Squares of the wave functions for isomer 1A superimposed on the MP2/aug-cc-pVDZ potential surface. Potential-energy contours are at energies 1.0, 2.0, 3.0, 4.0, 5.0, 6.0, 8.0, and 10.0 kcal/mol above the global energy minimum. (a) The ground state and (b) the first excited state are shown.

the 1-D model is 1.31 Å, as compared to the equilibrium value of 1.15 Å. In $n = 3$ clusters, $\langle R_{X-H1}\rangle_0$ is only slightly longer than the equilibrium distance, that is, about 0.04 Å. Thus, the quantum effects are large for $n = 1$ according to our calculations, but quantum effects are considerably smaller for $n \geq 2$.

From the energy difference between the ground state and the first excited state, the frequency for the periodic proton motion has been determined. The anharmonic proton-stretching frequencies can be calculated using the two-state model, as shown in our previous paper on the $N_2H_7^+$ cluster.[12] We argued that the proton vibrational behavior is mainly influenced by the two lowest eigenstates using the wave-packet dynamics of the 1-D model.[12] Calculated frequencies, ZPEs, and energies of first excited states are given in Table 5. For isomer 0A, the harmonic spectrum has a large, intense proton-stretching band at 2249 cm^{-1}, in contrast to the experimental frequency[26] of 1371 cm^{-1} for the corresponding vibration.

Del Bene and Jordan[11] also investigated the anharmonicity of the $ClH:NH_3$ complexes without water molecules using MP2/aug-cc-pVDZ potential-energy surfaces. They have pointed out that the harmonic treatment for $ClH:NH_3$ leads to a significant overestimation of the experimental proton-stretching frequency and that an anharmonic treatment improves the results. In their study, a 1-D potential curve was generated by the displacement vector of the normal coordinate for the harmonic proton-stretching mode and the two coordinates considered in the 2-D model were the H−X bond length and the N−H bond length. Our 1-D model gives a significantly improved result. The calculated frequency is 1328 cm^{-1} in the present model, whereas Del Bene et al. obtained 1842 cm^{-1}. In the 2-D model, their computed anharmonic proton-stretching frequency of 1566 cm^{-1} is close to our result of 1538 cm^{-1}. The differences in frequency between our calculation and the experimental data are 43 and 167 cm^{-1} in the 1-D and 2-D models, respectively. These differences are smaller than those of the previous study.[11]

TABLE 4: Expectation Values of Bond Lengths $\langle R_{X-H1}\rangle_0$ (Å) and Peak Bond Lengths r_{X-H1}^{max} (Å) Calculated by Using 1-D and 2-D Models Together with Optimized Equilibrium Bond Distances r_{X-H1eq} (Å) Obtained from Ab Initio MO Calculations Using an MP2/aug-cc-pVDZ Level of Theory

	parameter[a]	0A	1A	2A	2B	3A	3B
1-D	$\langle R_{X-H1}\rangle_0$	1.41	1.31	1.13	1.19	1.10	1.11
	r_{X-H1}^{max}	1.38	1.25	1.11	1.16	1.09	1.09
2-D	$\langle R_{X-H1}\rangle_0$	1.40	1.27				
	r_{X-H1}^{max}	1.39	1.25				
r_{X-H1eq}		1.34	1.15	1.08	1.11	1.06	1.07

[a] X = Cl for isomer 0A and X = N for other isomers.

TABLE 5: Frequencies (cm^{-1}), ZPEs (kcal/mol) by Harmonic and Anharmonic Approximations for Proton-Stretching Modes, and Energies (kcal/mol) of the First Excited State

	0A	1A	2A	2B	3A	3B
			Frequency			
harmonic	2249	1604	2624	2100	2797	2747
anharmonic						
one-dimensional	1328	552	1562	1108	2146	1947
two-dimensional	1538	790				
experimental[a]	1371					
			ZPE			
harmonic	3.2	2.3	3.8	3.0	4.0	3.9
anharmonic						
one-dimensional	2.6	1.4	2.9	2.4	3.6	3.4
$\Delta E_{harm.-anharm.}$	0.6	0.9	0.9	0.6	0.4	0.5
			First Excited State			
harmonic	9.6	6.9	11.4	9.0	12.0	11.7
anharmonic						
one-dimensional	6.4	3.0	7.4	5.6	9.7	9.0
$\Delta E_{harm.-anharm.}$	3.2	3.9	4.0	3.4	2.3	2.7

[a] Reference 26.

It is clear that anharmonic treatments lower the calculated vibrational frequencies. Although differences of the ZPEs between the harmonic and the anharmonic treatments are less than 1.0 kcal/mol, energy discrepancies for first excited states range from 2.3 to 4.0 kcal/mol. These facts suggest that the dominant factor in the lowering of vibrational frequencies is the lowering of the energies of the first excited states.

4. Conclusions

We have investigated the quantum effects of the proton motion on single proton-transfer reactions in small ammonia−hydrogen chloride clusters $NH_3:HCl:(H_2O)_n$ ($n = 0-3$) by using an ab initio MP2/aug-cc-pVDZ level of theory. Three new stable structures and one transition-state structure are investigated for these clusters. According to component analyses of intermolecular interactions, we have concluded that three-body terms make a significant contribution to the interaction potentials for the clusters.

The wave functions of the proton have been estimated by diagonalizing 1-D- and 2-D-model Hamiltonian matrices. Quantum effects of the proton motion lower the proton-stretching vibrational frequencies, especially for the most stable isomer in $n = 1$ clusters. Thus, the quantum effects are large for $n = 1$, according to our calculations, but they are much smaller for $n \geq 2$. In other words, complexes with just one water molecule result in a significant quantum delocalization of the proton.

Now, we can summarize structural features of NH_3:HCl:$(H_2O)_n$ ($n = 0-3$) clusters. In classical terms, the structure 0A exists as a hydrogen-bonded structure. Two conformations become stable in $n = 1$; one is a hydrogen-bonded structure, and the other is an ion-pair form. It is reasonable to say that the most stable isomer for $n = 1$ is the ionic structure, although it is weakened by the quantum effects of the proton motion. The lowest energy structures for the $n = 2$ and 3 clusters are also ionic. Quantum delocalization of the proton is much smaller for these clusters.

Acknowledgment. T.A. gratefully acknowledges Professor Neil Snider of Northwestern University, who assisted in the preparation of this manuscript. T.A. also thanks Professor Kazuo Kitaura for valuable comments and suggestions. Calculations were carried out at the Research Center for Computational Science in the Okazaki Research Facilities for the National Institutes of Natural Sciences.

References and Notes

(1) Biczysko, M.; Latajka, Z. *J. Chem. Phys.* **1999**, *313*, 366.
(2) Snyder, J. A.; Cazar, R. A.; Jamka, A. J.; Tao, F.-M. *J. Phys. Chem. A* **1999**, *103*, 7719−7724.
(3) Angle, L.; Stace, A. J. *J. Chem. Phys.* **1998**, *109*, 1713−1715.
(4) Ye, L.; Cheng, H.-P. *J. Chem. Phys.* **1998**, *108*, 2015−2023.
(5) Cheng, H.-P. *J. Chem. Phys.* **1996**, *105*, 6844.
(6) Scheiner, S.; Harding, L. B. *J. Am. Chem. Soc.* **1981**, *103*, 2169−2173.
(7) Jaroszewski, L.; Lesyng, B.; McCammon, J. A. *THEOCHEM* **1993**, *283*, 57−62.
(8) Cazar, R.; Jamka, A.; Tao, F.-M. *Chem. Phys. Lett.* **1998**, *287*, 549−552.
(9) Cazar, R. A.; Jamka, A. J.; Tao, F.-M. *J. Phys. Chem. A* **1998**, *102*, 5117−5123.
(10) Stich, I.; Marx, D.; Parrinello, M.; Terakura, K. *J. Chem. Phys.* **1997**, *107*, 9482.
(11) Del Bene, J. E.; Jordan, M. J. T. *J. Chem. Phys.* **1998**, *108*, 3205−3212.
(12) Asada, T.; Haraguchi, H.; Kitaura, K. *J. Phys. Chem. A* **2001**, *105*, 7423−7428.
(13) Li, R.-J.; Li, Z.-R.; Wu, D.; Hao, X.-Y.; Li, Y.; Wang, B.-Q.; Tao, F.-M.; Sun, C.-C. *Chem. Phys. Lett.* **2003**, *372*, 893−898.
(14) Komatsuzaki, T.; Iwao, O. *Mol. Simul.* **1996**, *16*, 321−344.
(15) Shimizu, A.; Tachikawa, H. *Chem. Phys. Lett.* **1999**, *314*, 516−521.
(16) Del Bene, J. E.; Jordan, M. J. T.; Gill, P. M. W.; Buckingham, A. D. *Mol. Phys.* **1997**, *92*, 429.
(17) Goodwin, E. J.; Howard, N. W.; Legon, A. C. *Chem. Phys. Lett.* **1986**, *131*, 319.
(18) Howard, N. W.; Legon, A. C. *J. Chem. Phys.* **1988**, *88*, 4694.
(19) Frish, M. J.; Trucks, G. W.; Schlegel, H. B.; Gill, P. M. W.; Scuseria, G. E.; Robb, M. A.; Cheeseman, J. R.; Strain, M. C.; Burant, J. C.; Stratmann, R. E.; Dapprich, S.; Kudin, K. N.; Millan, J. M.; Daniel, A. D.; Petersson, G. A.; Montgomery, J. A.; Zakrzewski, V. G.; Raghavachari, K.; Ayala, P. Y.; Cui, Q.; Morokuma, K.; Foresman, J. B.; Cioslowski, J.; Ortiz, J. V.; Barone, V.; Stefanov, B. B.; Liu, G.; Liashenko, A.; Piskorz, P.; Chen, W.; Wong, M. W.; Andres, J. L.; Replogle, E. S.; Gomperts, R.; Martin, R. L.; Fox, D. J.; Keith, T.; AlLaham, M. A.; Nanayakkara, A.; Challacombe, M.; Peng, C. Y.; Stewart, J. P.; Gonzales, C.; Head-Gordon, M.; Gill, P. M. W.; Johnson, B. G.; Pople, J. A. *Gaussian98*; Gaussian Inc.: Pittsburgh, PA, 1998.
(20) Dunning, T. H., Jr. *J. Chem. Phys.* **1989**, *90*, 1007.
(21) Kendall, R. A.; Dunning, T. H., Jr.; Harrison, R. J. *J. Chem. Phys.* **1992**, *96*, 6796.
(22) Woon, D. E.; Dunning, T. H., Jr. *J. Chem. Phys.* **1993**, *98*, 1358.
(23) Del Bene, J. E.; Shavitt, I. *THEOCHEM* **1994**, *307*, 27.
(24) Salvador, P.; Paizs, B.; Duran, M.; Suhai, S. *J. Comput. Chem.* **2001**, *22*, 765.
(25) Cristian, A. C.; Krylov, A. I. *J. Chem. Phys.* **2003**, *118*, 10912.
(26) Barnes, A. J.; Beech, T. R.; Mielke, Z. *J. Chem. Soc., Faraday Trans. 2* **1984**, *80*, 455.